OPEN ACCESS

University of BRISTOL

Garrad, M., Rossiter, J., & Hauser, H. (2018). Shaping Behavior With Adaptive Morphology. *IEEE Robotics and Automation Letters*, *3*(3), 2056-2062. https://doi.org/10.1109/LRA.2018.2807591

Peer reviewed version

Link to published version (if available):
10.1109/LRA.2018.2807591

Link to publication record in Explore Bristol Research
PDF-document

This is the author accepted manuscript (AAM). The final published version (version of record) is available online via IEEE at https://ieeexplore.ieee.org/document/8294256/. Please refer to any applicable terms of use of the publisher.

University of Bristol - Explore Bristol Research
General rights

This document is made available in accordance with publisher policies. Please cite only the published version using the reference above. Full terms of use are available:
http://www.bristol.ac.uk/red/research-policy/pure/user-guides/ebr-terms/

Shaping Behaviour with Adaptive Morphology

Martin Garrad[1,2], Jonathan Rossiter[1] and Helmut Hauser[1]

***Abstract*—Robots which exploit their embodiment promise to be more robust, energy-efficient and adaptable. However, the majority of systems designed in this way are only capable of exploiting their embodiment when performing a single task in a single environment. For such robots to be capable of adapting to a range of tasks or environments, they must be capable of adjusting their morphology on-line and have an understanding of how adjustments in both control and morphology affect their behaviour. We introduce the concept of the control-morphology (CM) space and the Variable Stiffness Swimmer (VSS), a multi-segment pendular robot with adaptive joint stiffness. This system allows us to perform an initial investigation into how navigating the CM space affects the behaviour of a robot. We show that the behaviour of the system is not only the result of selecting a particular location within the control-morphology space, but also the route taken to arrive at that point. We also demonstrate locations within the space where a shift in behaviour can be caused entirely by smooth on-line changes in morphology.**

***Index Terms*—Biologically-Inspired Robots; Underactuated Robots; Biomimetics**

I. INTRODUCTION

THE behaviour of a robot is the result of the dynamic interaction between the system's controller, and body and the environment [3], [4]. Given a particular task and environment, the standard approach is to first design a body and then try to find the appropriate controller for the system [5]. If a different behaviour is desired, the change is achieved by adjusting the control parameters. This approach has been successful when applied to automated assembly lines [6], autonomous drones [7] and self-driving cars [8]. However, for tasks which require interaction with the environment (for example walking or grasping), the resulting control problems often prove too complex [3].

An alternative approach comes from the philosophy of embodied intelligence [9], [10]. This places renewed focus on the design of the body, showing that in many cases complex control problems can be drastically simplified by appropriate choice of morphology. Examples include dynamic walkers [11], [12] and universal grippers [13].

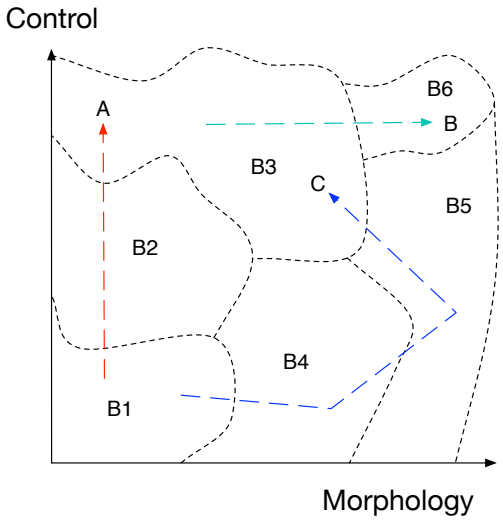

Fig. 1: The control-morphology space. The space defined by the control and morphology parameters can be partitioned into a number of behaviours. Traditional robot design picks a particular point on the morphology axis and then explores the control-space (For example, path A). The opposite approach, of fixing a control input and exploring morphology (path B) has recently been explored by Corruci et al. [1], [2]. To fully utilise all possible behaviours in the control-morphology space, it is likely to be necessary to make adjustments in both control and morphology parameters (path C).

Since both control and morphology affect behaviour, we can define a joint space, which we refer to as the control-morphology (CM) space (See Figure 1) . If we have N control parameters and M morphology parameters, the resulting CM space will have dimension $M + N$. The CM space of a system can be divided into a number of regions, with each region corresponding to a distinct behaviour. Changes in control or morphology parameters which do not cross a behavioural boundary, lead to changes in performance, but do not alter the overall behaviour. For example, a running robot will continue to run, albeit with increased speed or reduced stability. Alternatively, a change in parameters which crosses a boundary leads to a qualitative change in behavioural mode. For example, a running robot may begin to walk or hop.

If a system has the ability to vary a property of its morphology, it is reasonable to ask whether that property should still be considered a part of the robot morphology, or whether it should now be considered a part of the control system. In this work, we argue that such properties can be classified based

Manuscript received: September, 10, 2017; Revised Novemver, 28, 2017; Accepted January, 27, 2018

This paper was recommended for publication by Editor Yu Sun upon evaluation of the Associate Editor and Reviewers' comments. This work was supported by the EPSRC Centre for Doctoral Training in Future Robotics and Autonomous Systems (FARSCOPE) EP/L015293/1. Rossiter is supported by EPSRC grants EP/M026388/1 and EP/M020460/1. Hauser is supported by Leverhulme Trust Project RPG-2016-345.

[1]Martin Garrad, Jonathan Rossiter and Helmut Hauser are with the with the SoftLab, Bristol Robotics Laboratory, University of Bristol and University of the West of England, Bristol BS16 1QY, U.K `m.garrad@bristol.ac.uk`

[2]Martin Garrad is also with the EPSRC Centre for Doctoral Training in Future Autonomous and Robotic Systems (FARSCOPE), University of Bristol and University of the West of England

Digital Object Identifier (DOI): see top of this page.

upon how frequently they are changed. We argue that a typical control system will have a characteristic frequency, at which it updates the variables it is responsible for. Variables which are updated at a much lower frequency may be considered properties of the morphology. For example, in a standard PD control system, we would consider the demanded torque to be a control variable, but the control gains would be considered part of the morphology. On the other hand, in an optimal control approach, in which the gains may be scheduled at a rate comparable to the motor torques, these properties would both be considered control parameters.

To achieve autonomy, robotic systems must be capable of optimising behaviours for a particular task and environment, switching between multiple behaviours in response to a change in task, or maintaining a particular behaviour in response to a changing environment. The classical control approach, in which a single morphology is used for multiple tasks often requires significant complexity in the controller. Introducing additional degrees of freedom into the problem may appear to only increase the complexity of the problem. However, as these properties will only be updated infrequently, we argue that it is possible that the complexity of the controller can in fact be reduced if morphology is adapted in such a way that the natural dynamics of the system become more suitable for the task [14], [15]. Furthermore, it may be that a change in behaviour is achieved more elegantly or efficiently by an adjustment of morphology, rather than a change in controller. Similarly, maintenance of a particular behaviour in a changing environment may be more easily achieved via adjustments in morphology than in control parameters.

For robots to be given the ability to navigate the control-morphology space they must have the capacity to adapt their morphology on-line. Furthermore, they must have a higher level *behavioural controller* which understands how following a particular route through the control-morphology space will affect behaviour. The high dimensionality and complex structure of this space makes understanding it a challenge, further complicated by the fact that this space will change with changes in environment. Our approach here is to consider the CM space for a simple system in a single environment as a starting point.

In this paper, we explore the control-morphology space for an under-actuated multi-segment eel-like robot. We show that this simple system has multiple behaviours, and that these behaviours are a result of a particular choice of control and morphology parameters. We show that the behaviour of the system depends not only on the choice of these parameters, but the route through control-morphology space to reach them. Finally, we show that the system is capable of switching its behaviour on-line via smooth changes in morphology only.

There are a large number of similar multi-link pendular robots already reported in the literature [16], [17], [18]. Many of these robots use a servo motor at each joint. These systems approach the problem from the viewpoint of classical control and do not exploit the dynamics of the body-environment interaction. More closely related are the investigations of fish locomotion that utilise passive foils [19]. These studies have investigated the role of joint stiffness, however their approach is from a viewpoint of understanding the biomechanics of fish, rather than an investigation of the behavioural possibilities of a robotic system. Most closely related to this work is *Wanda*, the passive swimming robot [20], [21]. *Wanda* has been used to investigate behaviour optimisation via changes in morphology, but not the possibility of qualitative changes in behaviour. Finally, Corucci et al [1], [2] have explored changing behaviour via changes in morphology alone (See Figure 1, pathway B). In this work, a control input was fixed and a genetic algorithm was used to explore the morphology-behaviour space of an underwater legged robot.

On the control theory side, there are a number of approaches which optimise certain properties of the morphology of a system. These can broadly be divided into two categories. Firstly, there are methods which aim to optimise certain parameters of the morphology prior to the construction of the robot ([**?**]). These parameter values are likely to lose their optimality if the task or environment is changed. Secondly, there are approaches such as variable impedance control [22], [23], which take a morphology parameter and turn it into a controlled degree of freedom ([24], [25]). In these cases, the adaptation of morphology can lead to significantly more energy-efficient and safer behaviour, at the expense of increasing the complexity of the control problem.

This paper proceeds by first introducing the variable stiffness swimmer (VSS), an under-actuated swimming robot with adaptive joint stiffness. We present an overview of the mechanical design and characterise the ability to adjust joint stiffness. Next, we show that the behaviour of the system is affected by both the control parameters and morphology. We identify a number of behaviours and the transition points between these behaviours in control space. Finally, we investigate how we can change behaviour by navigating the CM space and show that there are certain regions in which changes in morphology alone are enough to cause qualitative changes in behaviour and that the behaviour of a system depends not only upon our final destination in CM space, but also the route taken to get there. We end with a discussion of the benefits of understanding the CM space for a robotic system and further areas for investigation.

II. The Variable Stiffness Swimmer

The variable stiffness swimmer (VSS) is an eel-inspired swimming robot. It is a four-link pendulum with torsional springs at each joint. The top module is sinusoidally driven at a specified frequency (f) and amplitude (A) by a servo motor (Dynamixel AX-12A, Robotis, South Korea), with the remaining modules passive. A stiffness adjustment mechanism is attached to each joint, enabling dynamic adjustment of joint compliance. Joint position is measured by a hall-effect sensor (Melexis MLX90316KDC, Mouser Electronics), mounted directly above the joint axis. Figure 2 shows the assembled robot.

A. Stiffness Adjustment

Joint stiffness is controlled by an adapted version of the MACCEPA [26] mechanism. Figure 3 shows an overview

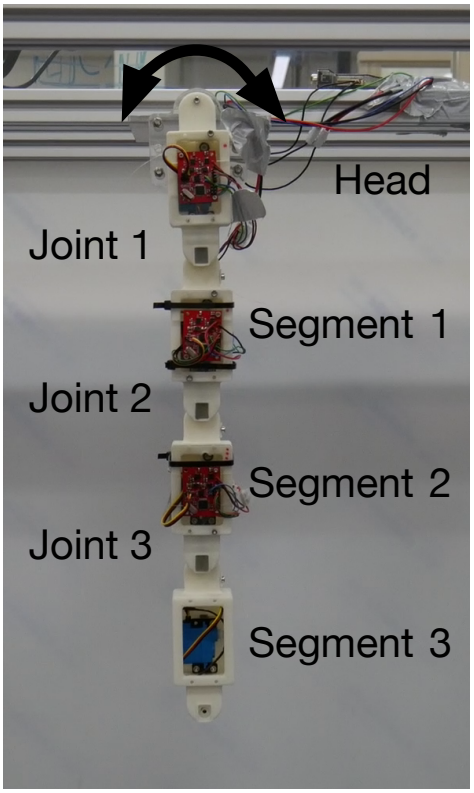

Fig. 2: The variable stiffness swimmer. The head is driven by a motor, while the remaining segments are passive. Joint stiffness is adjusted by a MACCEPA [26] inspired mechanism inside each segment.

of this mechanism. Stiffness of the link is controlled by adjusting the pretension P on the spring ($K_{spring} = 0.39\frac{N}{mm}$, LEM080CF 02S, Lee Springs, UK) via an embedded servo motor. The joint stiffness can be approximated by the expression:

$$K_\tau = P.\frac{k.B.C}{|B-C|} \tag{1}$$

where B and C represent the dimensions specified in Figure 3. Figure 4 shows the construction of a single segment of the VSS with the MACCEPA mechanism visible.

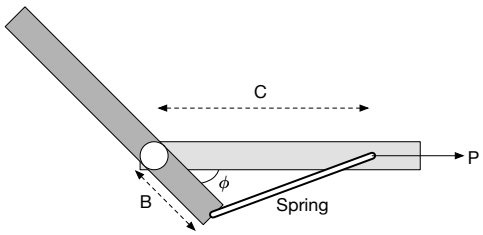

Fig. 3: The MACCEPA mechanism [26] . A spring attached between the two links provides a restoring force if the two links are not parallel to each other. By increasing the pretensioning force on the spring, the stiffness of the joint can be adjusted.

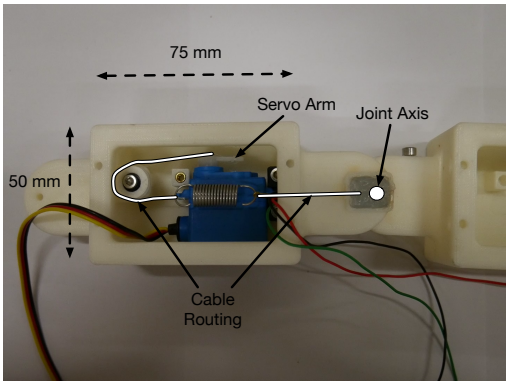

Fig. 4: A single VSS module.

B. Characterization of Stiffness Change

In order to assess the range of joint stiffnesses achievable by our system, we measured the relationship between restoring torque and angle for a number of spring pre-tensions. Joint angle was measured by the integrated hall-effect sensor, while torque was measured with a load cell (Vishay Tedea Huntleigh 1022, USA). We define relative pretension as:

$$RelativePretension = \frac{P}{P_{max} - P_{min}} \tag{2}$$

Figure 5 shows that joint stiffness can be approximately doubled, from an initial stiffness of $0.030\frac{N}{\circ}$ to a maximum stiffness of $0.056\frac{N}{\circ}$.

III. Results

In order to understand the control-morphology space of the VSS, we investigate how its behaviour is affected by both control inputs (driving frequency, f, and amplitude, A) and morphology (in this context, the joint stiffnesses, K_1, K_2, K_3).

To fully assess the impact of such changes, we would need to investigate how they affect ecologically significant properties such as swimming speed or energy efficiency. However, as the preliminary behavioural assessment is performed in air with the system fixed to rigid frame, it is necessary to identify summary statistics which we believe are related to these performance metrics.

We follow Ziegler et al. [27] in using the kinematic intensity as representative statistics of the system's behaviour. The

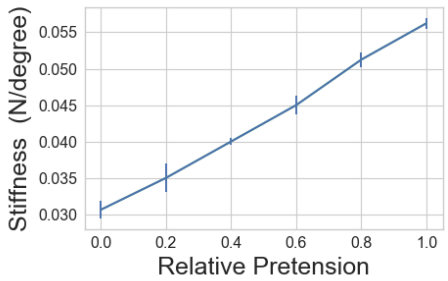

Fig. 5: Joint stiffness against relative pretension.

kinematic intensity (KI) is the magnitude of the difference between the maximum and minimum value of a particular variable over a single cycle.

For the VSS, we consider the mean kinematic intensity of the angles between each joint as the Lighthill model of fish locomotion [28] suggests these have a strong influence on swimming velocity. In the case of the final link, this corresponds to the tail beat angle.

In all experiments, we drive the system in air with a sinusoidal control input given by $\phi_0 = Asin(2\pi ft)$, where ϕ_0 represents the angle between the head and the body. The servo is fixed to a rigid frame meaning that all energy is transferred to the body of the VSS. Joint stiffnesses K_i are varied from $0.03\frac{N}{\circ}$ to $0.056\frac{N}{\circ}$. In total, this means our CM space is 5-dimensional $< f, A, K_1, K_2, K_3 >$. We begin by analysing the frequency response of the system in its most compliant state (exploring in a manner equivalent to path A in Figure 1) . This yields a number of fundamental behaviours. Next, we show that for certain fixed control inputs, the choice of morphology determines the resulting behaviour (exploring in a manner equivalent to path B in Figure 1) . Finally, we show that on-line changes in morphology can be used to drive a change in behavioural mode and investigate routes through the CM space.

A. Control-Behaviour-Space

Visual observation of the VSS suggests that it has four distinct behavioural modes, each with a characteristic body shape. Figure 6 shows time domain plots of the joint angles alongside key-frames for each mode. We confirm these modes quantitatively by observing that each has a characteristic set of phase relationships between joints. We also note that the transitions between modes occur at frequencies which maximise or minimise the frequency response.

Figure 7 shows the frequency response of the VSS in its most compliant state with a driving amplitude of 5 degrees. At the smallest amplitude and low frequencies (mode 1), the system behaves as a double pendulum around the first joint, with the three body joints in phase with each other. This behaviour has a resonant peak at $1Hz$. Increasing the frequency to $2.3Hz$ causes a transition to a second mode (mode 2) in which the bottom two links now oscillate in-phase with the head, while the first body links remains out of phase. This increase in frequency also leads to a significant increase in tail-beat intensity. Further increasing the frequency causes a transition to a third mode (mode 3), in which the middle body link is in phase with the first link and out of phase with the final body link. Finally, further increasing the frequency causes the system to transition to a fourth mode (mode 4) where the phase alternates between each link.

The frequency response analysis was then repeated at driving amplitudes of 9, 12, 15 and 19 degrees. Figure 8 shows the control space of the VSS partitioned into the four behavioural modes. Table I summarises the transition frequencies. In general, increasing the driving amplitude slightly reduces the transition frequencies. For the transitions between higher modes ($f_{2\to3}$, $f_{3\to4}$), the amplitude dependence diminishes above 12 degrees. Transitions frequencies for the higher modes at the largest amplitude were not found due to over-heating of the servo-motor.

TABLE I: Transition frequencies for the VSS in its most compliant state at a range of driving amplitudes. High-amplitude and high-frequency transitions not recorded due to motor-overheating.

Amplitude	$f_{1\to2}$ (Hz)	$f_{2\to3}$ (Hz)	$f_{3\to4}$ (Hz)
5°	2.3	3.9	4.2
9°	2.2	3.5	3.8
12°	2.1	3.4	3.7
15°	2	3.4	3.7
19°	1.9	N/A	N/A

B. The Effect of Morphology

The investigation of the influence of changes in control parameters on behaviour above has identified 4 behaviour modes and three key points: the (frequency, amplitude) tuples at which the system transitions between modes. These points represent landmarks in the control-morphology space. To understand the influence of morphology, we repeated the frequency analysis above at a range of morphologies (i.e joint stiffnesses). We drove the system at a driving frequency of 15 degrees. We considered stiffening of each joint individually (K_1, K_2, K_3), and stiffening of multiple joints simultaneously (K_{1+2+3}). Each joint is tested at stiffnesses 0.03, 0.035, 0.04, 0.045 and 0.05. The largest value of joint stiffness is not tested in order to prevent damage to the MACEPPA motor.

Figure 9 shows the transition frequencies ($f_{1\to2}$, $f_{2\to3}$, and $f_{3\to4}$) against both individual and simultaneous increases in joint stiffness. In all cases, increasing joint stiffness has a small effect on the transition frequency $f_{1\to2}$, and a greater effect on the transition frequency $f_{3\to4}$. In the case of the transition between the second and third modes, $f_{2\to3}$, increasing the stiffness of joints 1 or 2 appears to decrease the transition frequency, while increasing stiffness of joint 3 increases the transition frequency. Interestingly, in the case of simultaneous increases in joint stiffness, $f_{2\to3}$ increases, suggesting the influence of the third link's stiffness is stronger than that of the first two joints.

These results confirm that the behaviour of the VSS depends on both the influence of control and morphology parameters. Although the impact of the morphology is less than that of the control parameters, this is likely due to the smaller range of variation possible for morphology. Unlike biological systems which can adjust stiffness through several orders of magnitude, the VSS is limited to a far smaller range of stiffnesses (a factor of two).

C. On-line navigation of the Control-Morphology space

Initial investigation of the control-morphology space of the VSS identified a number of locations where a shift in behavioural mode can be achieved by adjusting either frequency, driving amplitude or morphology of the system. However, in the previous experiments, the system was allowed to return to a resting state between episodes. In most real-world contexts,

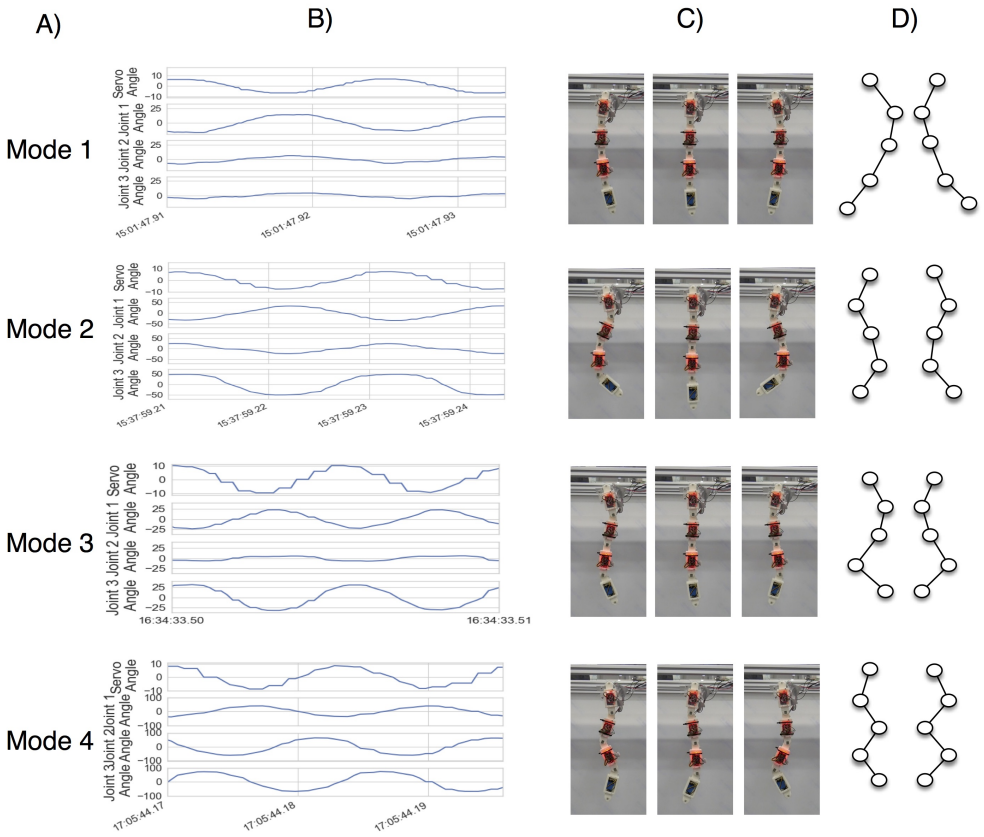

Fig. 6: An overview of the VSS's behavioural modes. Column A) lists the mode, while B) shows a time-domain plot of the joint angles for two oscillation cycles. We note that each mode has a characteristic set of phase relationships. Column C) shows key-frames corresponding to each mode, while D) shows a schematic representation of the mode.

this is likely to be undesirable. Robotic systems should be capable of smoothly adjusting behaviour on-line. In this section, we show that the behaviour of a system is not just the result of a particular place within the CM space, but also depends on the route taken through it.

Figure 10 shows two routes through the CM-space. In the path a), the system increases the amplitude (OA) of oscillation past the transition amplitude $A_{1\to2}$ and enters behavioural mode 2. At this point, the system stiffens (AB) and then reduces the oscillation amplitude below the transition point (BC). However, the system remains in mode 2. In the second path (Figure 10b), the system stiffens (OC), increases oscillation amplitude (CB) above the transition point $A_{1\to2}$ of the first path and then reduces stiffness. However, the system remains in mode 1 throughout. This demonstrates that the behaviour of a system is not just the result of a particular parameter setting, but also the path taken through the control-morphology space.

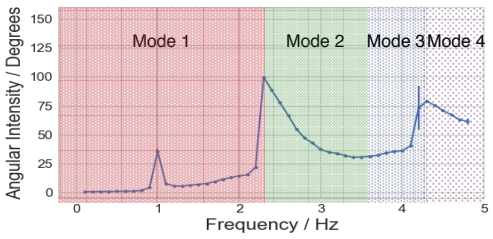

Fig. 7: Frequency response of the VSS in its most compliant state driven at an amplitude of 5 degrees. The plots show the tail beat intensity of the VSS as frequency is increased. Shaded areas indicate the different behavioural modes.

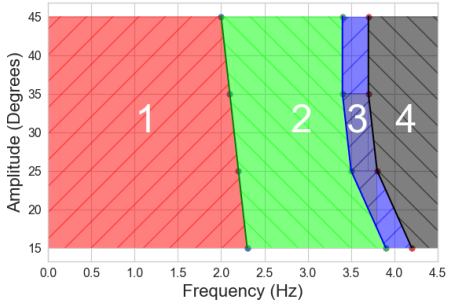

Fig. 8: The control space of the VSS. Each colored region represents a different behavioural mode.

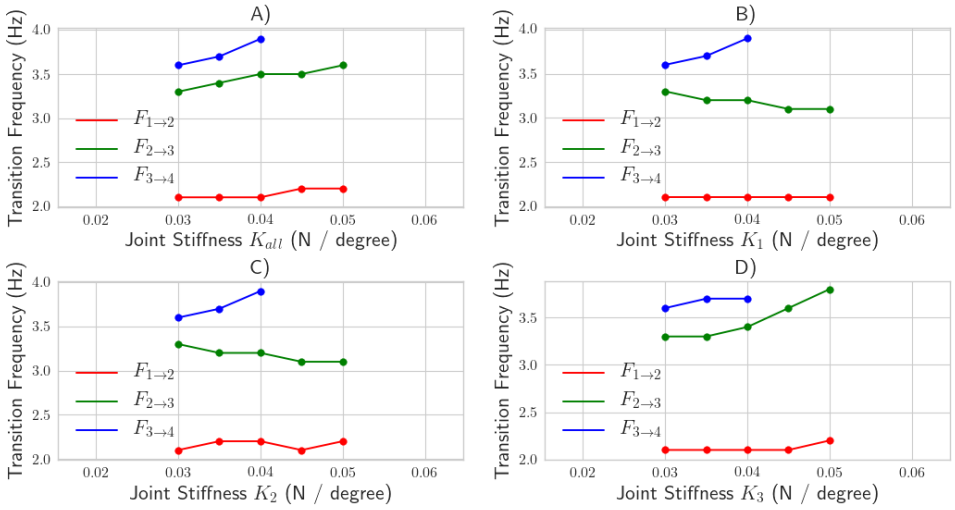

Fig. 9: Transition frequencies ($f_{1\to2}$, $f_{2\to3}$, and $f_{3\to4}$) against joint stiffness. A) shows the effect of increasing the stiffness of all joints simultaneously, while B), C), and D) show the effect of increasing the stiffness of joints 1, 2, and 3 separately.

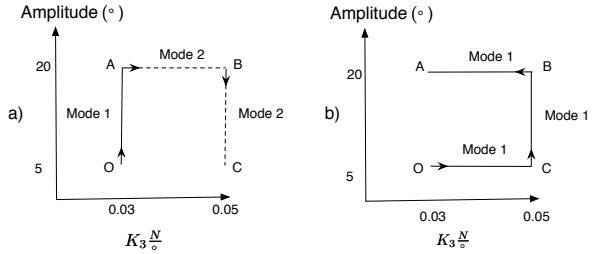

Fig. 10: Two routes through the VSS CM space. In a), the system increases oscillation amplitude (OA), transitioning to mode 2. The system then stiffens (AB) and decreases oscillation amplitude (BC), remaining in mode 2. In b), the system stiffens (OC), increases oscillation amplitude (CB) and then reduces stiffness (BA). However, it remains in mode 1 throughout.

Although this hysteresis complicates our understanding of the control-morphology space, it may be a desirable property for such a system. Gait transitions such as walking to running incur an energetic cost. Thus it is important that a robotic system does not have a sharp transition point between gaits as this can lead to a form of chattering where the system alternates between nearby gaits. Furthermore, extreme points in the control-morphology space may optimise important metrics such as speed or efficiency. For example, the transition frequencies identified in the frequency analysis above match the resonant frequencies for their corresponding modes. The hysteresis in gait transitions allows the system to remain at these locations in control-morphology space without danger of transitioning to a different mode.

D. Switching Behaviour With Morphology

We now show that it is possible to change behaviour online via changes in morphology only. Figure 11 shows a time-domain plot of the VSS driven at a frequency of $2Hz$ and

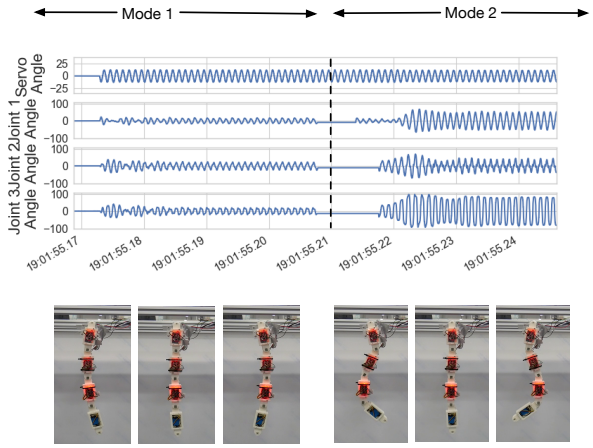

Fig. 11: Time-domain plots of the VSS driven at $2Hz$ and 18 degrees. The stiffness of the third link is changed at t_{switch}, as indicated by dashed black line. This changes causes a switch from mode 1 into mode 2. Key-frames from the corresponding modes shown below.

an amplitude of 18 degrees. At T_{switch}, the stiffness of the third joint is decreased from its $0.05\frac{N}{°}$ to $0.03\frac{N}{°}$. This shift causes the transition from mode 2 to mode 1. Supplementary materials S1 shows a video of the VSS transitioning in this manner.

IV. Discussion & Conclusions

The behaviour of a robot can be adjusted by altering the parameters of its controller, morphology or both together. We have introduced the concept of the control-morphology space and the VSS as a platform for investigating this space. We have demonstrated that the behaviour of a dynamic system is affected not only by its location within this space, but also by its route through the space. We have also shown that

there are certain locations within this space where changes in morphology alone can switch behaviour.

In general, for a robotic system to be able to adaptively produce intelligent behaviours, it will require some degree of complexity. A key decision for the designer of a robotic system is how to distribute this complexity. The standard approach to building a robot places the majority of the complexity in the control and planning subsystems, with morphology generally kept simple. Embodied systems minimise control complexity, but in doing so sacrifice the ability to adapt their behaviour. The VSS has shown that adaptive morphology can allow embodied systems to adapt their behaviour in a qualitative manner. The added complexity inherent in this approach is two fold. Firstly, mechanisms which allow adaptation of morphology increase the complexity of the body. Furthermore, the high-dimensionality and path-dependence of behaviour demonstrated by the VSS suggests that the higher level *behavioural controller* will also need some degree of complexity.

The next target for the VSS is to investigate how movement through control-morphology space effects performance in terms of ecologically important measures such as swimming velocity and energy efficiency. Thus, the next steps for this work is to complete a thorough investigation of the control-morphology space in air (considering for example, a greater range of anisotropic stiffnesses) and then proceed to investigate how changes in environment (for example fluids of varying viscosity and granular media of varying grain size) impact upon the features of the control-morphology space. Finally, we are using a simple model of the system to investigate metrics to for quantifying the cost of taking a particular route through control-morphology space. This will allow us to quantify the optimal route through the space to either force or prevent a shift in behaviour as the environment changes.

ACKNOWLEDGEMENT

All data in the paper is available on the University of Bristol's research database, data.bris.ac.uk/data under the DOI: to follow.

REFERENCES

[1] F. Corucci, M. Calisti, H. Hauser, and C. Laschi, "Evolutionary discovery of self-stabilized dynamic gaits for a soft underwater legged robot," in *Advanced Robotics (ICAR), 2015 International Conference on*. IEEE, 2015, pp. 337–344.

[2] ——, "Novelty-based evolutionary design of morphing underwater robots," in *Proceedings of the 2015 annual conference on Genetic and Evolutionary Computation*. ACM, 2015, pp. 145–152.

[3] R. Pfeifer, F. Iida, and G. Gómez, "Morphological computation for adaptive behavior and cognition," in *International Congress Series*, vol. 1291. Elsevier, 2006, pp. 22–29.

[4] R. Pfeifer, M. Lungarella, and F. Iida, "Self-organization, embodiment, and biologically inspired robotics," *Science*, vol. 318, no. 5853, pp. 1088–1093, 2007.

[5] R. Pfeifer, F. Iida, and J. Bongard, "New robotics: Design principles for intelligent systems," *Artificial life*, vol. 11, no. 1-2, pp. 99–120, 2005.

[6] T. Brogårdh, "Present and future robot control developmentan industrial perspective," *Annual Reviews in Control*, vol. 31, no. 1, pp. 69–79, 2007.

[7] D. Mellinger and V. Kumar, "Minimum snap trajectory generation and control for quadrotors," in *Robotics and Automation (ICRA), 2011 IEEE International Conference on*. IEEE, 2011, pp. 2520–2525.

[8] S. Thrun, M. Montemerlo, H. Dahlkamp, D. Stavens, A. Aron, J. Diebel, P. Fong, J. Gale, M. Halpenny, G. Hoffmann, *et al.*, "Stanley: The robot that won the DARPA grand challenge," *Journal of field Robotics*, vol. 23, no. 9, pp. 661–692, 2006.

[9] J. Buchli and A. J. Ijspeert, "Self-organized adaptive legged locomotion in a compliant quadruped robot," *Autonomous Robots*, vol. 25, no. 4, pp. 331–347, 2008.

[10] R. Pfeifer, F. Iida, and M. Lungarella, "Cognition from the bottom up: on biological inspiration, body morphology, and soft materials," *Trends in cognitive sciences*, vol. 18, no. 8, pp. 404–413, 2014.

[11] D. Owaki, M. Koyama, S. Yamaguchi, S. Kubo, and A. Ishiguro, "A two-dimensional passive dynamic running biped with knees," in *Robotics and Automation (ICRA), 2010 IEEE International Conference on*. IEEE, 2010, pp. 5237–5242.

[12] R. Tedrake, T. W. Zhang, and H. S. Seung, "Learning to walk in 20 minutes," in *Proceedings of the Fourteenth Yale Workshop on Adaptive and Learning Systems*. Yale University New Haven (CT), 2005, pp. 1939–1412.

[13] J. R. Amend, E. Brown, N. Rodenberg, H. M. Jaeger, and H. Lipson, "A positive pressure universal gripper based on the jamming of granular material," *IEEE Transactions on Robotics*, vol. 28, no. 2, pp. 341–350, 2012.

[14] H. Hauser, "Morphological computation - a potential solution for the control problem in soft robotics," in *Advances in Cooperative Robotics*. World Scientific, 2017, pp. 757–764.

[15] H. Hauser and F. Corucci, "Morphosis taking morphological computation to the next level," in *Soft Robotics: Trends, Applications and Challenges*. Springer, 2017, pp. 117–122.

[16] C. D. Onal and D. Rus, "Autonomous undulatory serpentine locomotion utilizing body dynamics of a fluidic soft robot," *Bioinspiration & biomimetics*, vol. 8, no. 2, p. 026003, 2013.

[17] T. Sato, T. Kano, and A. Ishiguro, "A snake-like robot driven by a decentralized control that enables both phasic and tonic control," in *Intelligent Robots and Systems (IROS), 2011 IEEE/RSJ International Conference on*. IEEE, 2011, pp. 1881–1886.

[18] A. J. Ijspeert, A. Crespi, D. Ryczko, and J.-M. Cabelguen, "From swimming to walking with a salamander robot driven by a spinal cord model," *Science*, vol. 315, no. 5817, pp. 1416–1420, 2007.

[19] G. V. Lauder, B. Flammang, and S. Alben, "Passive robotic models of propulsion by the bodies and caudal fins of fish." *Integrative & Comparative Biology*, vol. 52, no. 5, 2012.

[20] M. Ziegler, F. Iida, and R. Pfeifer, "Cheap underwater locomotion: roles of morphological properties and behavioural diversity," in *International Conference on Climbing and Walking Robots, CLAWAR, Karlsruhe*, 2006.

[21] M. Ziegler, M. Hoffmann, J. P. Carbajal, and R. Pfeifer, "Varying body stiffness for aquatic locomotion," in *Robotics and Automation (ICRA), 2011 IEEE International Conference on*. IEEE, 2011, pp. 2705–2712.

[22] N. Hogan, "Impedance control: An approach to manipulation," in *American Control Conference, 1984*. IEEE, 1984, pp. 304–313.

[23] C. Della Santina, M. Bianchi, G. Grioli, F. Angelini, M. Catalano, M. Garabini, and A. Bicchi, "Controlling soft robots: balancing feedback and feedforward elements," *IEEE Robotics & Automation Magazine*, vol. 24, no. 3, pp. 75–83, 2017.

[24] V. Duindam and S. Stramigioli, "Optimization of mass and stiffness distribution for efficient bipedal walking," in *Proceedings of the International Symposium on Nonlinear Theory and Its Applications*, 2005.

[25] D. Braun, M. Howard, and S. Vijayakumar, "Optimal variable stiffness control: Formulation and application to explosive movement tasks," *Autonomous Robots*, vol. 33, no. 3, pp. 237–253, 2012.

[26] R. Van Ham, B. Vanderborght, M. Van Damme, B. Verrelst, and D. Lefeber, "Maccepa, the mechanically adjustable compliance and controllable equilibrium position actuator: Design and implementation in a biped robot," *Robotics and Autonomous Systems*, vol. 55, no. 10, pp. 761–768, 2007.

[27] M. Ziegler and R. Pfeifer, "Sensory feedback of a fish robot with tunable elastic tail fin," in *Conference on Biomimetic and Biohybrid Systems*. Springer, 2013, pp. 335–346.

[28] M. Lighthill, "Large-amplitude elongated-body theory of fish locomotion," *Proceedings of the Royal Society of London. Series B, Biological Sciences*, pp. 125–138, 1971.